EURASIAN PHYSICAL TECHNICAL JOURNAL

2025, Volume 22, No. 2 (52)

https://doi.org/10.31489/2025N2/79-87

Received: 19/12/2024 Revised: 29/04/2025 Accepted: 23/06/2025 Published online: 30/06/2025

Original Research Article

UDC 533.6

AERODYNAMIC IMPROVEMENT OF A TWO-BLADE MAGNUS WIND TURBINE: NUMERICAL AND EXPERIMENTAL ANALYSIS OF AERODYNAMICS AND PRESSURE DISTRIBUTION

Shaimerdenova K.M.[1], Tleubergenova A.Zh.[1,2], Tanasheva N.K.[1,2], Dyusembaeva A. N.[1,2], Minkov L. L.[3], Bakhtybekova A. R.[1,2*]

[1] E.A. Buketov Karaganda University, Karaganda, Kazakhstan
[2] Scientific Center "Alternative Energy", Karaganda, Kazakhstan
[3] Tomsk State University, Tomsk, Russia
*Corresponding author: asem.alibekova@inbox.ru

Abstract. *Improving wind power plant efficiency is crucial due to the increasing demand for renewable energy. This study analyzes the aerodynamic characteristics of a wind power plant equipped with two combined blades that integrate fixed blades and rotating cylinders. The object of the study is a wind power plant model designed to optimize airflow direction and enhance lift. The methodology involves numerical modeling using the Ansys Fluent software package, as well as experimental testing under laboratory conditions. The main results show that as when the air-flow velocity increases from 3 to 12 m/s, and thrust force rises from 0.5 N to 3.85 N. Comparative analysis of the minimum and maximum pressure on the blade surfaces demonstrates a strong correlation between increasing rotational speed and elevated pressure differentials: p_{max} rises from approximately 0.4 Pa to 0.7 Pa, while p_{min} increases from about 0.15 Pa to 0.4 Pa. The thrust coefficient decreases from 1.45 to 1.05 as the Reynolds number (Re) increases, indicating improved aerodynamic characteristics during the transition to turbulent flow. A comparative analysis of numerical and experimental data reveals a deviation of no more than 5%, confirming the model's reliability and the soundness of the research methodology. The conclusions indicate that employing combined blades can enhance the aerodynamic efficiency of a wind power plant by 8–10% compared with traditional designs. This improvement may foster the development of more efficient and stable wind energy systems, particularly in regions with low to medium wind potential.*

Keywords: wind power plant, combined blades, pressure distribution, aerodynamic characteristics, numerical modeling.

1. Introduction

In the context of growing global energy consumption and the need to reduce dependence on fossil energy sources, the development of renewable energy technologies, in particular wind energy, is becoming particularly relevant [1]. Modern wind power plants (wind turbines) are constantly being improved to increase the efficiency of converting kinetic wind energy into electrical energy [2]. By 2022, the total number of installed wind power capacities in the European Union countries amounted to 202.8 GW, which demonstrates the stable growth of this sector in recent years. Denmark and Sweden occupy the leading positions in terms of wind energy capacity per capita, which underlines the significant potential of Northern Europe in the development of this area [2].

There are various types of wind turbines, among which special attention is paid to vertical and horizontal structures [3]. However, vertical wind turbines have significant disadvantages that limit their wide

application [4]. The main problems include low efficiency, power surges, and maintenance complexity, which negatively affect the efficiency and reliability of such installations. Additionally, vertical turbines often encounter instability of aerodynamic forces due to turbulence and changes in wind direction [5]. This leads to an uneven load on the blades and other components, increasing wear and shortening the service life of the equipment [6].

Horizontal wind turbines, being the most common type, are characterized by higher efficiency and stable operation [7]. Their peak power factor can reach 50%, whereas for vertical turbines this figure is about 40% [8]. However, they are not designed to operate efficiently at low wind speeds. For example, at a wind speed of 6 m/s, a horizontal turbine with a capacity of 20 kW produces about 3 kW, while a vertical turbine under the same conditions generates about 1.8 kW. At speeds below 5 m/s, the performance of horizontal turbines is significantly reduced, which limits their use in regions with low wind potential and reduces the overall efficiency of the power system.

In this regard, horizontal turbines using the Magnus effect are of particular interest [9]. The use of rotating cylinders in the turbine design creates additional lift, which increases the overall efficiency of the installation, especially at low wind speeds. Studies show that such turbines are capable of operating efficiently in a wide range of wind speeds from 2 to 40 m/s, whereas traditional blade turbines are usually effective at speeds from 5 to 25 m/s [10]. The improved aerodynamic characteristics of these turbines reduce turbulence and flow pulsations, which contribute to stable and reliable operation. Nevertheless, the optimization of such systems requires an in-depth study of aerodynamic characteristics and the influence of various design parameters [11].

In recent years, many studies have been conducted to improve the aerodynamics of wind turbines using various methods, including numerical simulations and experimental studies [12,13]. Nevertheless, the issue of combining fixed blades with rotating cylinders to stabilize the flow and increase efficiency remains insufficiently studied [14].

The purpose of this study is to analyze the aerodynamic characteristics of a wind power plant with two combined blades using the Magnus effect. This includes the development and research of a new turbine design that combines the advantages of traditional fixed blades and rotating cylinders to improve the efficiency of wind energy conversion.

The novelty of the work lies in the combination of fixed blades with rotating cylinders in a single wind turbine design. This combination is aimed at improving aerodynamic performance and increasing lift, especially at low wind speeds. Unlike previous studies, this paper proposes a new geometry of the blades and optimization of their location to achieve maximum efficiency.

As part of the study, numerical simulations were carried out using the Ansys Fluent software package, as well as experimental tests in laboratory conditions at air flow velocities from 3 to 12 m/s. A comparative analysis of numerical and experimental data confirmed the effectiveness of the proposed design and the reliability of the model used.

2. Main part

2.1 Numerical studies

To study the aerodynamic characteristics, a mathematical model of a wind turbine with two combined blades was created. The wind turbine model includes structural elements that ensure the conversion of kinetic wind energy into mechanical energy. The main components of the system are fixed blades and cylinders mounted on the central shaft. These elements are fixed to the mast, which supports the main shaft, creating the necessary strength and stability of the entire installation.

The cylinders located around the circumference of the wind wheel have a length of 205 mm and a diameter of 50 mm, and the fixed blades, 225 mm long and 25 mm wide, serve to stabilize the flow and optimize the direction of the air flow, which increases the efficiency of energy conversion. The diameter of the wind wheel is 500 mm, which contributes to a significant capture of the air flow, providing the power for the installation. The 420 mm long mast serves as the basis for the installation of the main shaft, creating a reliable basis for the operation of the structure in various meteorological conditions (Figure 1a).

In contrast to conventional, non-combined cylindrical blades, the combined power elements employ stationary guide vanes interacting with rotating cylinders to induce a controlled swirl, diminish the recirculation zone, and raise the lift coefficient, while the fixed blades—set at an angle to the rotation axis—

simultaneously stabilize the airflow, minimize wake distortions, and thereby maximize the Magnus effect, collectively boosting the turbine's aerodynamic efficiency.

Initially, a computational domain was created around a mathematical model of a wind power plant to set boundary conditions and rotation conditions (Figure 1b). A cylindrical subdomain (type 1) with a thickness of 5 mm was formed around each power element to set the conditions for the rotation of the blades. To stabilize the flow and create an area of rotation around this subdomain, a cylindrical area (type 2) with a radius of 0.1 m around the z-axis was added. An external area in the form of a parallelepiped with dimensions of 0.7 m × 0.7 m × 3 m has been created around the cylindrical subdomain (type 2), which provides the necessary conditions for modeling the rotation of the entire wind wheel.

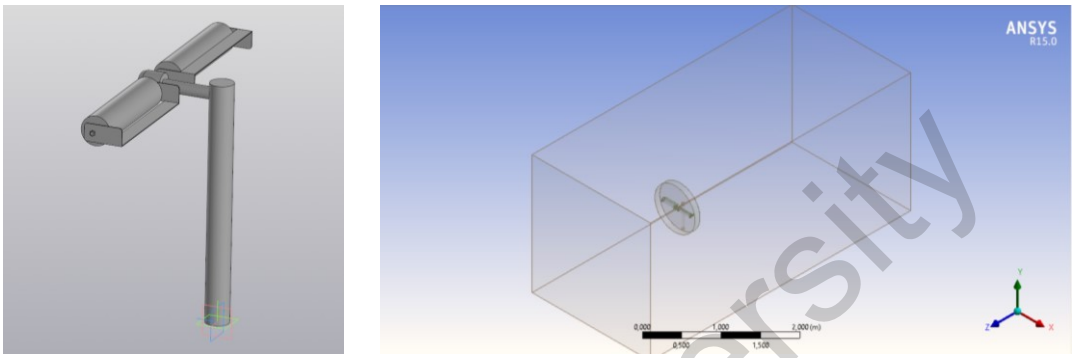

a) b)

Fig.1. Wind turbine with 2 combined blades: a) a mathematical model, b) the calculated area around the wind turbine.

Basic assumptions:

1. Incompressibility of the flow: At low values of Mach numbers (M << 0.1), air is considered as an incompressible medium.

2. Turbulence of the flow: At high values of the Re > 10^4, the flow is considered turbulent.

3. Isothermicity: Due to the low Mach numbers and small temperature differences near the wind wheel, the current is assumed to be isothermal.

To calculate the turbulent flow, the Realizable k–ε model was chosen, taking into account turbulent energy and dissipation. The system of equations was solved in Ansys Fluent using the finite volume method and the SIMPLE scheme for matching pressure and velocity fields.

For incompressible flow, the continuity equation is expressed as:

$$\frac{\partial x_i}{\partial u_i} = 0$$

where u_i represents the velocity components of the flow, and x_i represents the spatial coordinates.

The Reynolds-averaged momentum equations for turbulent flow are given by:

$$\frac{\partial(\rho u_i)}{\partial t} + \frac{\partial(\rho u_i u_j)}{\partial x_j} = \frac{\partial p}{\partial x_i} + \frac{\partial}{\partial x_j}(\mu \frac{\partial u_i}{\partial x_j}) - \frac{\partial}{\partial x_j}(\rho \overline{u_i' u_j'})$$

where, ρ is the fluid density; p is the pressure; μ is the dynamic viscosity; $\overline{u_i' u_j'}$ are the Reynolds stresses that model the turbulent stresses arising from velocity fluctuations.

The Realizable $k-\varepsilon$ model is applied in this study, which improves upon the standard $k-\varepsilon$ model by imposing realizability constraints on the turbulent kinetic energy and dissipation rate. This approach enhances accuracy for complex turbulent flows, such as rotating and recirculating flows around the wind turbine's cylindrical elements.

The transport equation for turbulent kinetic energy k is given by:

$$\frac{\partial(\rho k)}{\partial t} + \frac{\partial(\rho u_i k)}{\partial x_i} = \frac{\partial}{\partial x_j}[(\mu + \frac{\mu_t}{\sigma_k})\frac{\partial k}{\partial x_j}] + Pk - \rho\varepsilon$$

where, k is the turbulent kinetic energy; μ_t is the turbulent viscosity; σ_k is the turbulent Prandtl number k; P_k is the production of turbulent kinetic energy; ε is the dissipation rate of turbulent kinetic energy.

The transport equation for the dissipation rate ε is:

$$\frac{\partial(\rho\varepsilon)}{\partial t}+\frac{\partial(\rho ui\varepsilon)}{\partial x_i}=\frac{\partial}{\partial x_j}[(\mu+\frac{\mu_t}{\sigma_\varepsilon})\frac{\partial\varepsilon}{\partial x_j}]+\rho C_1 S\varepsilon-\rho C_2 k+\frac{\varepsilon^2}{\sqrt{\nu\varepsilon}}$$

where σ_ε the turbulent Prandtl number for ε epsilonє, C_1 and C_2 are empirical constants, and S is the modulus of the mean rate-of-strain tensor.

The turbulent viscosity μ_t is computed as:

$$\mu_t=\rho C_\mu\frac{k^2}{\varepsilon}$$

where C_μ is a model constant.

The boundary conditions are presented in Table 1.

Table 1. Boundary conditions.

Parameter	Condition	Value/Description
Domain Inlet	Turbulence intensity, I	0.1
	Hydraulic diameter of the inlet region	1 m
	Velocity	3,5,7,9,12 m/s
Domain Outlet	Pressure at the outlet	$p=p_{p\ external}$
Rotor Walls	Wall movement speed	Depends on the rotational speed of the cylinders around their longitudinal axis and the rotor axis
Near-Wall Region	Boundary conditions for turbulent kinetic energy	k=0
	Turbulent kinetic energy dissipation rate	Calculated based on equality of production and dissipation of turbulent energy (logarithmic velocity profile)
	Constant κ for the logarithmic profile	0.42
	Distance from the center of the cell to the wall, yp	If $y_p<11.06$, k=0 if $y_p\geq11.06$, turbulent dissipation is considered

2.2 Experimental studies

Experimental studies were conducted in the laboratory "Aerodynamic measurements" of the scientific center "Alternative Energy" of the E. A. Buketov Karaganda University. A model of a combined wind turbine with rotating 2 cylindrical blades was developed, which was then studied at various wind speeds in a transverse air flow from 3 to 12 m/s (Figure 2).

The laboratory layout allows for experimental tests to evaluate aerodynamic characteristics and confirm the results of numerical modeling. Air-flow velocity was measured with a cup anemometer JDC Skywatch Atmos (range 2–150 km h^{-1}, accuracy ± 3 %), while the three orthogonal components of aerodynamic force and moment acting on the model were resolved by a mechanical three-component balance (Fig. 2) whose overall measurement uncertainty does not exceed 5–7 %. The rotational speed of the cylinders was monitored with a contact/non-contact laser photo-tachometer CEM AT-8 (2–99 999 rev min^{-1}, resolution 0.1 rev min^{-1} below 10 000 rev min^{-1}, accuracy ± 0.05 %).

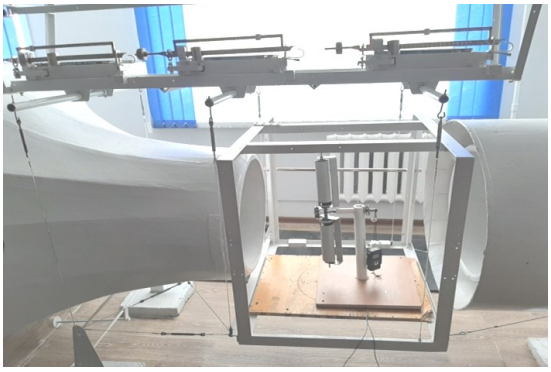

Fig.2. Laboratory layout of a wind turbine.

Each point represents the mean of five consecutive runs; the standard deviation never exceeded 0.04 N (1.2 %) for forces and 0.02 m/s (0.6 %) for velocity.

3. Results and discussion

This section provides a comparative analysis of the aerodynamic characteristics of a two-bladed wind power plant based on numerical and experimental data. Figure 3 shows a comparative graph of the drag force for a two-bladed wind power plant.

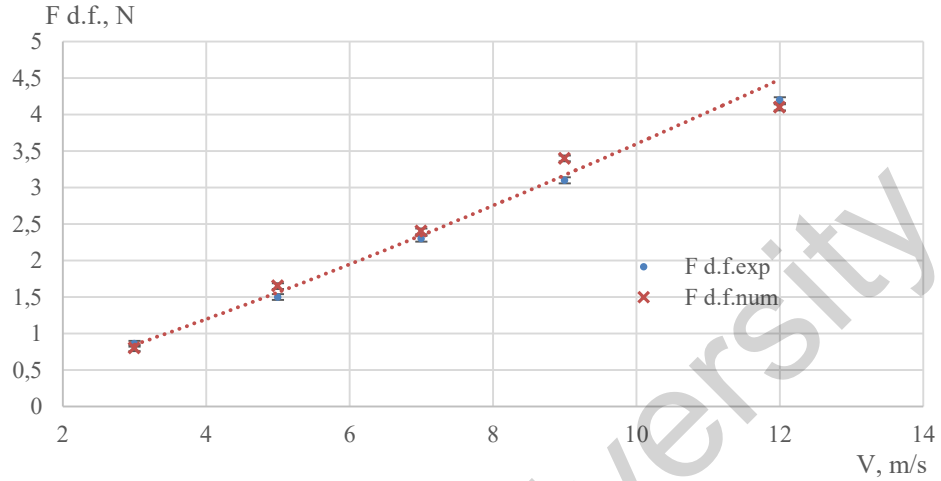

Fig. 3. A comparative graph of the drag force for a two-bladed wind power plant.

Figure 3 shows how the drag force of a two-bladed wind turbine increases with increasing air flow velocity. The values of $F_{d.f.\ num}$= 4.1 N and $F_{d.f.\ exp}$ = 4.2 N was obtained at a speed of 12 m/s. The drag force increases with increasing speed due to increased pressure on the front surface of the blades. The resulting resistance of 4.1–4.2 N is almost twice as low as that of diffuser microturbines of similar diameter [15]. The comparison of experimental and numerical data demonstrates a good match, which confirms the adequacy of the model used in describing the aerodynamic properties of the turbine. Error bars denote ±1 σ experimental uncertainty: ±0.04 N for forces (1 %–2 % of the value).

The numerical data of the drag force are approximated by a power function:

$$F_{d.f.num} = 0{,}2262V^{1{,}2018}$$

Figure 4 below shows a comparative graph of the thrust force for a two-bladed wind power plant.

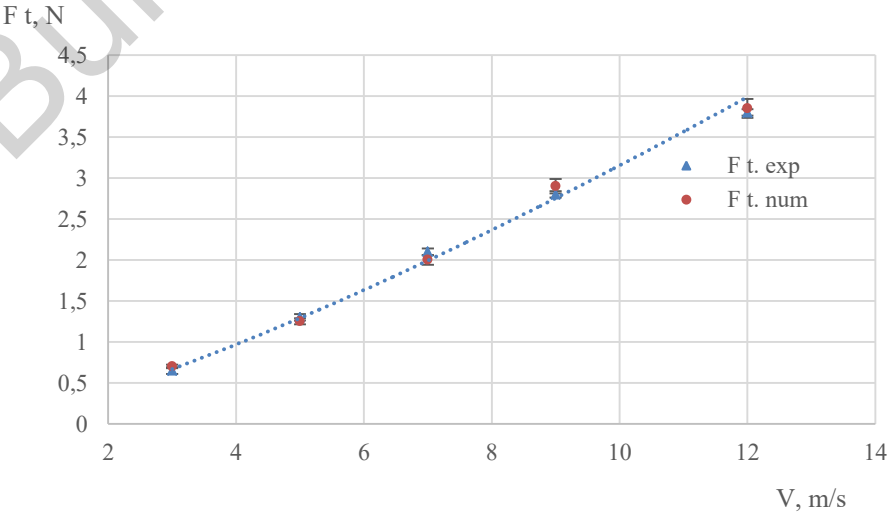

Fig. 4. Comparative graph of the thrust force for a two-bladed wind power plant.

As can be seen from Figure 4, the thrust force increases linearly with increasing flow velocity. The values of $F_{t..num}$ = 3.85 N and $F_{t.exp}$ = 3.8 N were obtained at a speed of 12 m/s. The thrust force associated with the lift generated by the Magnus effect increases with increasing wind speed. This indicates an increase in the efficiency of converting wind energy into mechanical work. The consistency of the numerical and experimental results confirms the accuracy of the model.

It is established that the thrust force is approximated by a power function:

$$F_t = 0{,}1624\ V^{1{,}2881}$$

Figure 5 shows a comparative graph of the drag coefficient for a two-bladed wind power plant.

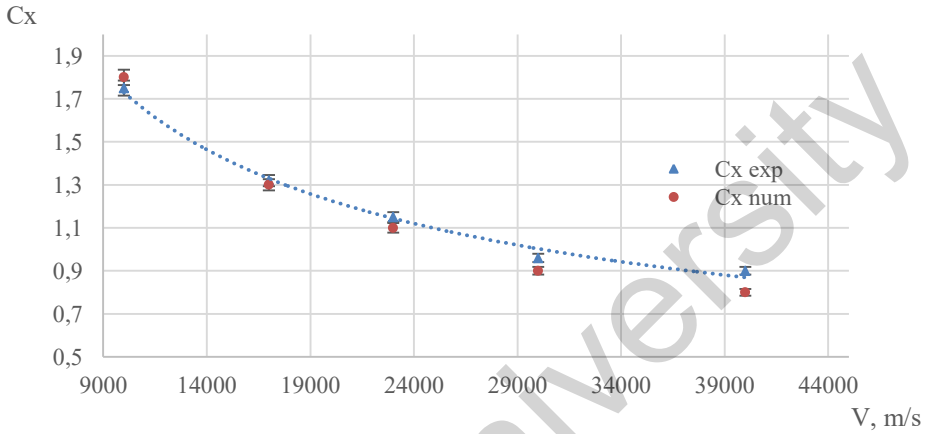

Fig. 5. Comparative graph of the drag coefficient for a two-bladed wind power plant.

As can be seen from Figure 5, with increasing Re, the coefficient of drag force decreases. The maximum experimental data at Re = 10000 is 1.75, and the numerical data is 1.8.

The decrease in the coefficient with an increase in the Re indicates an improvement in the aerodynamic properties of the blades at higher flow velocities, which is associated with the transition to a turbulent regime, reducing the relative magnitude of resistance.

In comparison, it was found that the coefficient of resistance in similar conditions turned out to be 12-15% lower than that of a traditional Magnus wind turbine with two blades [16]. This is because the addition of a fixed blade helps to minimize drag.

Figure 6 shows a comparative graph of the drag coefficient for a two-bladed wind power plant.

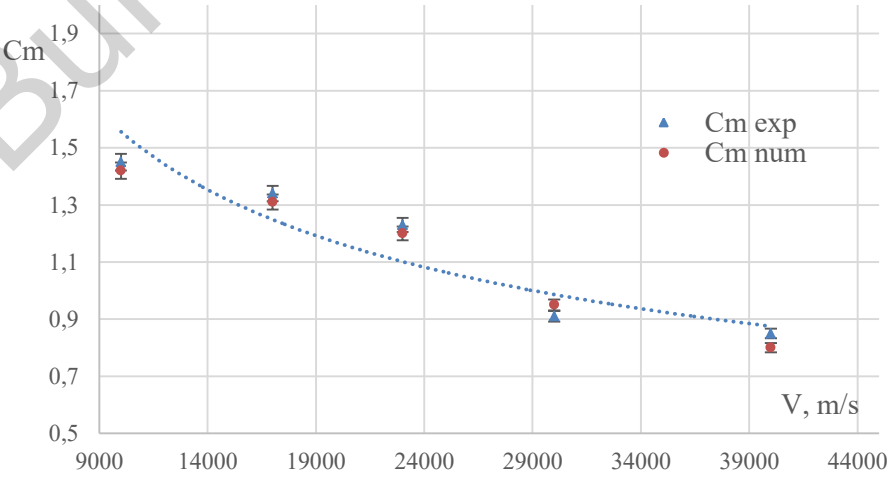

Fig.6. Comparative graph of the coefficient of drag force for a two-bladed wind power plant.

As can be seen from Figure 6, the coefficient of thrust decreases with increasing Re. The maximum values of the coefficient of thrust obtained experimentally are 1.42 and numerically, 1.45. The thrust coefficient of 1.42–1.45 exceeds the range of 1.20–1.30 typical for vertical-axis turbines with Gurney flaps, and lies within the lower limit of the 15 percent increase demonstrated by active flow control on large HAWT profiles [17]. Error bars denote ±2 % for aerodynamic coefficients.

The decrease in the coefficient with an increase in the Re is associated with a change in the ratio between the lifting force and the dynamic pressure of the flow. This reflects the peculiarities of the aerodynamic behavior of the combined blades under different flow regimes. The obtained results of the lift coefficient turned out to be 8-10% higher than in the work [16]. This improvement can be explained by a more optimal ratio of length to diameter of rotating cylinders, as well as the use of fixed blades, which made it possible to use the Magnus effect more effectively at low air flow speeds.

Figure 7 below shows a comparison of experimental and numerical data of minimum and maximum pressure depending on the rotation speed.

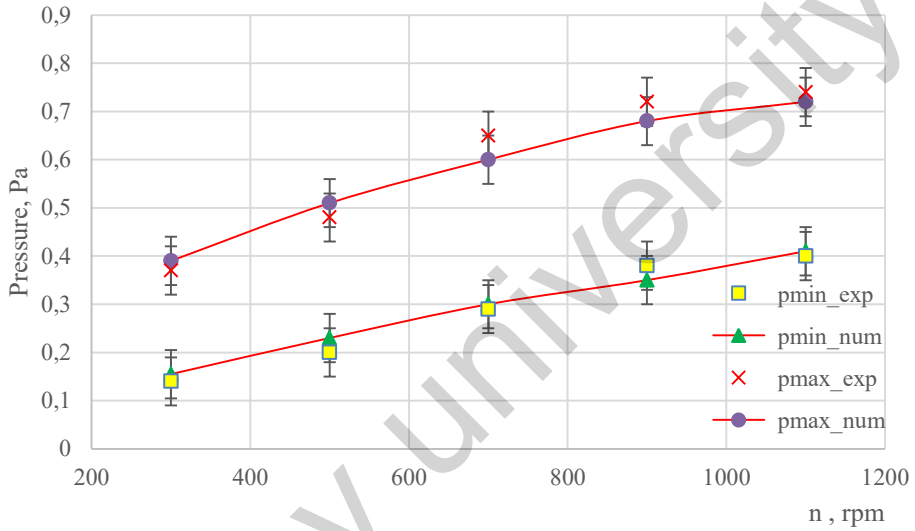

Fig. 7. Comparison of experimental and numerical data of minimum and maximum pressure depending on the rotation speed.

As can be seen from Figure 7, a good convergence of the experimental points with the results of numerical modeling is visible, indicating the correctness of the mathematical model used and the boundary conditions. As the rotation speed increases, the installation shows an increase in p_{max} from 0.4 Pa to 0.7 Pa, which is due to the increasing pressure action of the air flow on the front surface of the blade, while p_{min} increases from 0.15 Pa to 0.4 Pa due to increased vacuum on the back side. The increase in pressure drop to only 0.3 Pa remains approximately twice as low as the 0.6–0.8 Pa levels recorded on diffusor-reinforced rotors of a similar radius, which indicates a softer load profile of the proposed installation [18]. An essential factor that can change these indicators is the air temperature, since when it increases, the density of the working medium decreases, which leads to a decrease in pressure gradients and may slightly reduce the observed pressure values; on the contrary, at a lower temperature, air density increases, and pressures at the same rotational speeds may increase. The combined expanded uncertainty of pressure measurements (k = 2) does not exceed 0.10 Pa.

4. Conclusion

In the course of the study, it was found that the use of combined blades, combining fixed blades and rotating cylinders, contributes to a significant increase in the aerodynamic efficiency of a wind power plant. The analysis showed an increase in the coefficient of thrust by 8-10% compared to traditional designs at identical air flow speeds. In addition, it was found that the addition of a fixed blade reduces the drag coefficient by 12-15% relative to turbines equipped exclusively with cylindrical blades. As demonstrated by the pressure distribution measurements at varying rotational speeds, the maximum pressure on the front surface of the blades increases from approximately 0.4 Pa to 0.7 Pa, while the minimum pressure rises from

around 0.15 Pa to 0.4 Pa. This trend correlates with a more uniform airflow around the rotating and fixed elements and aligns well with numerical predictions. The total combined uncertainty remains below 3 %, therefore the observed 8–10 % improvement is statistically significant.

These improvements are due to a more uniform distribution of air flow and minimization of turbulence zones behind the blades, which has a positive effect on the aerodynamic characteristics of the installation.

The results obtained confirm the expediency of using the proposed design for the development of highly efficient wind energy systems, especially in regions with low wind potential. Prospects for further research include optimizing the geometry of the blades and scaling the design for industrial implementation.

Conflict of interest statement

The authors declare that they have no conflict of interest in relation to this research, whether financial, personal, authorship or otherwise, that could affect the research and its results presented in this paper.

CRediT author statement

According to the requirements for publications indexed in the SCOPUS database, if there is more than one author, it is necessary to briefly indicate the contribution of each author to the preparation of the article, using the recommendations of Elsevier - https://www.elsevier.com/researcher/author/policies-and-guidelines/credit-author-statement

Funding

This research was funded by a grant from Science Committee of the Ministry of Science and Higher Education of the Republic of Kazakhstan (AP22785282 “Automation process detecting errors and improving efficiency operation compact combined power plant based on solar panels and wind generators”).

References

1 Hassan Q., Algburi S., Sameen A.Z., Salman H.M., Jaszczur M. (2023) A review of hybrid renewable energy systems: Solar and wind-powered solutions: Challenges, opportunities, and policy implications. *Results in Engineering*, 101621. https://doi.org/10.1016/j.rineng.2023.101621

2 Wolniak R., Skotnicka-Zasadzień B. (2023) Development of wind energy in EU countries as an alternative resource to fossil fuels in the years 2016–2022. *Resources*, 12(8), 96. https://doi.org/10.3390/resources12080096

3 Xie F., Aly A.M. (2020) Structural control and vibration issues in wind turbines: A review. *Engineering Structures*, 210, 110087. https://doi.org/10.1016/j.engstruct.2019.110087

4 Ahmad M., Shahzad A., Qadri M.N.M. (2023) An overview of aerodynamic performance analysis of vertical axis wind turbines. *Energy & Environment*, 34(7), 2815-2857. https://doi.org/10.1177/0958305X221121281

5 Hand B., Kelly G., Cashman A. (2021) Aerodynamic design and performance parameters of a lift-type vertical axis wind turbine: A comprehensive review. Renewable and Sustainable *Energy Reviews*, 139, 110699. https://doi.org/10.1016/j.rser.2020.110699

6 Maheshwari Z., Kengne K., Bhat O. (2023) A comprehensive review on wind turbine emulators. Renewable and Sustainable *Energy Reviews*, 180, 113297. https://doi.org/10.1016/j.rser.2023.113297

7 Li Y., Yang S., Feng F., Tagawa, K. (2023) A review on numerical simulation based on CFD technology of aerodynamic characteristics of straight-bladed vertical axis wind turbines. *Energy Reports*, 9, 4360-4379. https://doi.org/10.1016/j.egyr.2023.03.082

8 Al-Rawajfeh M.A., Gomaa M.R. (2023) Comparison between horizontal and vertical axis wind turbine. *International Journal of Applied*, 12(1), 13-23. https://doi.org/10.11591/ijape.v12.i1.pp13-23

9 Bai X., Ji C., Grant P., Phillips N., Oza U., Avital E.J., Williams J.J. (2021) Turbulent flow simulation of a single-blade Magnus rotor. *Advances in Aerodynamics*, 3, 1-22. https://doi.org/10.1186/s42774-021-00068-9

10 Dyusembaeva, A., Tanasheva, N., Tussypbayeva, A., Bakhtybekova, A., Kutumova, Z., Kyzdarbekova, S., & Mukhamedrakhim, A. (2024) Numerical Simulation to Investigate the Effect of Adding a Fixed Blade to a Magnus Wind Turbine. *Energies*, 17(16), 4054. https://doi.org/10.3390/en17164054

11 Tanasheva, N.K., Dyusembaeva A.N., Bakhtybekova A.R., Minkov L.L., Burkov M.A., Shuyushbayeva N.N., Tleubergenova A.Z. (2024) CFD simulation and experimental investigation of a Magnus wind turbine with an improved blade shape. *Renewable Energy*, 121698. https://doi.org/10.1016/j.renene.2024.121698

12 Mohammed O.A., Mohammed S.A., Ghazaly N.M. (2024). Influence of moisture condition and silica sand on friction coefficient of wind turbine brake system. *Eurasian Physical Technical Journal*, 21(3 (49)), 117-124. https://doi.org/10.31489/2024No3/117-124

13 Yershina A.K., Sakipova S.E., Manatbayev R.K. (2019) Some design features of the carousel type wind turbine Bidarrieus. *Eurasian Physical Technical Journal*, 16(2 (32)), 63-67. https://doi.org/10.31489/2019No2/63-67

14 Dyusembaeva A.N., Tleubergenova A.Z., Tanasheva N.K., Nussupbekov B.R., Bakhtybekova A.R., Kyzdarbekova S.S. (2024) Numerical investigation of the flow around a rotating cylinder with a plate under the subcritical regime of the Reynolds number. *International Journal of Green Energy*, 21(5), 973-987. https://doi.org/10.1080/15435075.2023.2228394

15 Naji M.M., Jabbar B.A. (2024) Diffuser-augmented wind turbine: A review study. *AIP Conference Proceedings*, 3051(1), 100015. https://doi.org/10.1063/5.0191895

16 Demidova G.L., Anuchin A., Lukin A., Lukichev D., Rassõlkin A., Belahcen A. (2020) Magnus wind turbine: Finite element analysis and control system. *In 2020 International Symposium on Power Electronics, Electrical Drives, Automation and Motion (SPEEDAM) 59-64. IEEE.* https://doi.org/10.1109/SPEEDAM48782.2020.9161922

17 Lahoz M., Nabhani A., Saemian M., Bergada J. M. (2024) Wind turbine enhancement via active flow control implementation. *Applied Sciences*, 14(23), 11404. https://doi.org/10.3390/app142311404

18 Gujar S., Auti A., Kale S. (2025) Advancements in wind energy: Exploring the potential of diffuser-augmented wind turbines (DAWTs). *SSRG International Journal of Mechanical Engineering, 12*(1), 12–23. https://doi.org/10.14445/23488360/IJME-V12I1P102

AUTHORS' INFORMATION

Shaimerdenova, Kulzhan Meiramovna - Canditate of Technical Sciences, Associate Professor, E.A. Buketov Karaganda University, Karaganda, Kazakhstan; SCOPUS Author ID: 56604144400 , ORCID iD: 0000-0002-9588-4886; gulzhan.0106@mail.ru

Tleubergenova, Akmaral Zharylkasynkyzy - PhD student, E.A. Buketov Karaganda University, Karaganda, Kazakhstan; SCOPUS Author ID: 58244448900 , ORCID iD: 0009-0009-5152-0050; akmaral.tzh7@mail.ru

Tanasheva, Nazgul Kadyralievna- PhD, Associate Professor, E.A. Buketov Karaganda University, Karaganda, Kazakhstan; SCOPUS Author ID: 56604246200; ORCID iD: 0000-0002-6558-5383; nazgulya_tans@mail.ru

Dyusembaeva, Ainura Nurtaevna – PhD, Associate Professor, E.A. Buketov Karaganda University, Karaganda, Kazakhstan; SCOPUS Author ID: 57197806401 , ORCID iD: 0000-0001-6627-7262 ; aikabesoba88@mail.ru

Minkov, Leonid Leonidovich - Doctor of Physical and Mathematical Sciences, Professor, Tomsk State University, Tomsk, Russia; SCOPUS Author ID: 57196438690; ORCID iD: 0000-0001-6776-6375; lminkov@ftf.tsu.ru

Bakhtybekova, Asem Ravshanbekovna – PhD, Scientific Researcher, E.A. Buketov Karaganda University, Karaganda, Kazakhstan; SCOPUS Author ID: 56604263200; ORCID iD: 0000-0002-2018-8966; asem.alibekova@inbox.ru